

FUEL DEFORMATION IN A LOSS-OF-FLOW ACCIDENT IN THE GAS-COOLED FAST BREEDER REACTOR

T. R. WEHNER, D. T. EGGEN

*Department of Engineering Sciences, The Technological Institute,
Northwestern University, Evanston, Illinois 60201, U.S.A.*

This paper describes the development and results of the Northwestern University Fuel Rod Computer Code (NUFROD), a computer code for studying initial gross fuel deformation in an hypothetical loss-of-flow accident (LOF) in the gas-cooled fast breeder reactor (GCFR). The purpose of the study is to determine the mode of initial gross fuel deformation by examining the mechanical fuel behavior early in the transient. The manner in which the fuel breaks up can significantly alter later events in the accident sequence.

The mechanical model of NUFROD includes effects of temperature, pressure, fuel creep, and spatial variation of material properties. Fuel/cladding mechanical interaction is excluded because the cladding expands away from the fuel during a LOF. The columnar, equiaxed, and unstructured fuel zones are modeled and circumferential and axial stress discontinuities are accommodated at the fuel zone interfaces.

For simplicity and efficiency an analytic solution is used with the generalized plane strain approximation. The method of successive elastic solutions is used in conjunction with the Prandtl-Reuss flow laws and the von Mises yield criterion to calculate the stresses and strains during the reactor transient.

Three accidents with different coolant flow coastdown rates are examined. The results indicate that cladding melting and coastdown rate have a significant influence on the fuel stress state and the expected gross fuel deformation. Relatively fast transients can be expected to result in melting as the mode of gross fuel deformation. Relatively slow transients can be expected to result in fuel swelling or cracking. The interaction of stresses and fission gas in the fuel needs further investigation.

1. Introduction

The Northwestern University Fuel Rod Computer Code (NUFROD) was developed to study initial fuel behavior in a hypothetical loss-of-flow accident (LOF) without reactor shutdown in the gas-cooled fast breeder reactor (GCFR). The purpose of this study is to determine the mode of gross fuel deformation for different flow coastdown rates before loss of fuel pin geometry. Fuel stresses and strains are calculated for a representative high-powered fuel pin in the GCFR core during this transient undercooling accident. Conclusions are drawn from these calculated stresses. The effects of temperature, pressure, fuel creep and spatial variations in fuel materials are included in the analysis as is the thermal interaction of the fuel and cladding. Fuel/cladding mechanical interaction and reactivity feedback are excluded.

Mechanical interaction between the cladding and the fuel can reasonably be ignored in this transient because the stainless steel (SS316) 316 cladding thermally expands away from the fuel during the transient. For simplicity and efficiency an analytic solution is used for a small strain analysis in NUFROD. Plastic deformation from creep is included in a quasistatic fashion using the method of successive elastic solutions, the Prandtl-Reuss flow laws, and the von Mises yield criterion [1]. The sintered fuel pellet column is assumed to be restructured but uncracked.

2. Mechanical Analysis

The fuel pin is divided into axial segments with each axial segment subdivided into radial rings. This permits the use of an analytic solution for stresses and strains in a fuel pin having axially and radially varying properties. Thus the basic unit to be analyzed is a right circular annular cylinder chosen for uniform density, porosity, and grain size. No stress analysis is performed on the cladding in the LOF sequence because the cladding temperature increase is greater than that for the fuel, and the SS316 cladding has a larger coefficient of linear thermal expansion than the mixed-oxide fuel [2]. Thus, the force on the outer surface of the fuel comes from the gap pressure and not from the fuel/cladding mechanical interaction. In considering the thermal influence of the cladding on the fuel, it is assumed that once the cladding has melted at any axial segment it is swept down and away from the fuel by downward-flowing helium coolant.

The solution is obtained for an annular right circular cylinder with the generalized plane strain approximation [3]. The constitutive equations are

$$e_i = \frac{1}{E} \left[(1+\nu)\sigma_i - 3\nu\sigma_m \right] + e^{th} + e_i^c, \quad (1)$$

where i may refer to the radial, circumferential, or axial component, e_i is the total strain, E is Young's modulus, ν is Poisson's ratio, σ_i is the stress, σ_m is the mean stress, e^{th} is the isotropic linear thermal strain, and e_i^c is the creep strain. The thermal strain, e^{th} , is defined by

$$e^{th} = \int_{T_{ref}}^T \alpha(T') dT', \quad (2)$$

where α is the temperature-dependent instantaneous coefficient of linear thermal expansion, T is the temperature at which the thermal strain is to be evaluated, and T_{ref} is the reactor steady-state operating temperature. The constitutive eq. (1) is inverted with the condition of creep strain incompressibility, $e_r^c + e_\theta^c + e_z^c = 0$. The resulting expressions for stresses are

$$\sigma_i = 2G \left[e_i + \frac{3\nu}{(1-2\nu)} e_m - \frac{(1+\nu)}{(1-2\nu)} e^{th} - e_i^c \right], \quad (3)$$

where G is the shear modulus and e_m is the mean total strain.

The kinematic equations for generalized plane strain are

$$e_r = \frac{\partial u}{\partial r}, \quad (4)$$

$$e_\theta = \frac{u}{r}, \quad \text{and} \quad (5)$$

$$e_z = \text{constant}, \quad (6)$$

where r is radius and u is radial displacement. After the kinematic eqs. (4)-(6) are substituted into the inverted constitutive eq. (3), the expressions for stresses are substituted into the equilibrium equation

$$\frac{\partial \sigma_r}{\partial r} + \frac{(\sigma_r - \sigma_\theta)}{r} = 0 \quad (7)$$

The result is a second-order linear partial differential equation in u , radial displacement. The general solution for radial displacement as a function of radius is

$$u = \frac{(1+\nu)}{(1-\nu)} \frac{1}{r} \int_a^r e^{th} r' dr' - \frac{(1-2\nu)}{2(1-\nu)} \left[\frac{1}{r} \int_a^r e_z^c r' dr' - r \int_a^r \frac{(e_r^c - e_\theta^c)}{r'} dr' \right] + \frac{c_1}{r} + c_2 r, \quad (8)$$

where a is the inner radius of the cylinder and c_1 and c_2 are constants to be determined. This general solution for radial displacement is substituted back into the kinematic eqs. (4)-(6) and then into the inverted constitutive eq. (3) so that the pressure boundary conditions can be applied to determine the unknown constants.

The boundary conditions are

$$\sigma_r (r=a) = -p, \quad (9)$$

$$\sigma_r (r=b) = -q, \quad \text{and} \quad (10)$$

$$2\pi \int_a^b \sigma_z r dr = F_z, \quad (11)$$

where p is the pressure at the inner surface of the cylinder, q is the pressure at the outer surface of the cylinder, b is the outer cylinder radius, and F_z is the axial force on the cylinder. After the constants are determined and some algebraic manipulation has been done, the resulting expressions for the stresses as functions of radius are

$$\begin{aligned} \sigma_r = & - \frac{(b^2 q - a^2 p)}{(b^2 - a^2)} + \frac{(q-p)b^2 a^2}{(b^2 - a^2) r^2} + \frac{E}{(1-\nu)} \left[\left(1 - \frac{a^2}{r^2}\right) \frac{\langle e^{th} \rangle}{2} - \frac{1}{r^2} \int_a^r e^{th} r' dr' \right] \\ & + 2G \left[\left(1 - \frac{a^2}{r^2}\right) d + \frac{(1-2\nu)}{2(1-\nu)} \frac{1}{r^2} \int_a^r e_z^c r' dr' + \frac{1}{2(1-\nu)} \int_a^r \frac{(e_r^c - e_\theta^c)}{r'} dr' \right], \quad (12) \end{aligned}$$

$$\begin{aligned} \sigma_\theta = & - \frac{(b^2 q - a^2 p)}{(b^2 - a^2)} - \frac{(q-p)b^2 a^2}{(b^2 - a^2) r^2} + \frac{E}{(1-\nu)} \left[\left(1 + \frac{a^2}{r^2}\right) \frac{\langle e^{th} \rangle}{2} + \frac{1}{r^2} \int_a^r e^{th} r' dr' - e^{th} \right] \\ & + 2G \left[\left(1 + \frac{a^2}{r^2}\right) d - \frac{(1-2\nu)}{2(1-\nu)} \frac{1}{r^2} \int_a^r e_z^c r' dr' + \frac{1}{2(1-\nu)} \int_a^r \frac{(e_r^c - e_\theta^c)}{r'} dr' + \frac{\nu}{(1-\nu)} e_r^c - e_\theta^c \right] \quad (13) \end{aligned}$$

and

$$\sigma_z = \frac{-2\nu(b^2 - a^2)}{(b^2 - a^2)} + \frac{E}{(1-\nu)} (\nu \langle e^{th} \rangle - e^{th}) + 2G \left[2\nu d + \frac{\nu}{(1-\nu)} \int_a^r \frac{(e_r^c - e_\theta^c)}{r'} dr' + \frac{e_r^c}{(1-\nu)} + e_\theta^c \right] + E_{\theta z} \quad (14)$$

where $\langle e^{th} \rangle$ is defined as the areal average thermal strain and the constant d is defined by

$$d = \frac{-1}{4(1-\nu)} \left[(1-2\nu) \langle e_z^c \rangle + b^2 \langle e_r^c - e_\theta^c \rangle r^{-2} \right] \quad (15)$$

$\langle x \rangle$, the areal average of quantity x , is defined by

$$\langle x \rangle = \frac{2 \int_a^b x r dr}{(b^2 - a^2)} \quad (16)$$

where r is radius and a and b are the inner and outer radii of the right circular annular cylinder. From this analytic solution for a single cylinder, we can calculate the stresses in an axial segment that consists of many concentric annular cylinders. The solutions for the cylinders are joined at the cylinder interfaces by the continuity of radial displacement and radial force. In each axial segment, columnar, equiaxed, and unstructured fuel zones may exist. Within a fuel zone all stresses and strains are continuous. At radial fuel-zone interfaces creep strain discontinuities are permitted.

To calculate stresses and strains at the inner and outer surfaces of all the unit cylinders, the thermal strain and the creep strains are assumed to be linear functions of radius. Boundary conditions for each unit cylinder must be obtained before the analytic solution can be used. The expression for radial displacement of the outer surface of a unit cylinder is set equal to the expression for radial displacement of the directly-adjacent larger unit cylinder. The resulting nonsymmetric tridiagonal matrix equation can be solved for the "interface pressure" boundary conditions. Stresses and strains can then be determined anywhere along the radius of the axial segment.

3. Solution Technique

In the preceding section creep strains are assumed to be known at the unit cylinder interfaces. In practice the stresses and creep strains must be determined simultaneously. The method of successive elastic solutions [1] is used for this purpose. In this iterative solution process the Prandtl-Reuss flow laws and the von Mises yield criterion are used. The plastic strain-total strain equations are used to accelerate convergence [1],[4].

To calculate the solution at time $t+\Delta t$, where Δt is the time step size, the accumulated creep strains at time t must be known. At the start of the reactor transient, the fuel is assumed to be in a zero stress state with no accumulated creep strains. Temperature, thermal strains, and pressure boundary conditions at time $t + t$ are calculated. The radial and circumferential creep strain increments, Δe_r^c and Δe_θ^c , during the time step are initially guessed. The axial creep strain increment is equal to the opposite of the sum of the radial and circumferential increments by incompressibility. These increments are added to creep strains accumulated to time t , e_i^{ac} , using

$$e_i^c = e_i^{ac} + \Delta e_i^c \quad (17)$$

Total axial strain is calculated approximately by using areal-averaged mechanical properties. Unit cylinder "interface pressures" and then stresses are calculated. The modified deviatoric strains, e_i^m , defined by

$$e_i^m = e_i - e_m - e_i^{ac} \quad (18)$$

where e_m is the mean total strain, are calculated from

$$e_i^m = \frac{(\sigma_i - \sigma_m)}{2G} + \Delta e_i^c \quad (19)$$

This expression is obtained from the definition (18) and the constitutive eq. (1). The equivalent modified deviatoric strain, e_{eq}^m is calculated with

$$e_{eq}^m = \left\{ \frac{2}{3} \left[(e_r^m)^2 + (e_\theta^m)^2 + (e_z^m)^2 \right] \right\}^{1/2} \quad (20)$$

For steady-state creep the equivalent stress, σ_{eq} , is obtained from the solution to

$$\frac{\sigma_{eq}}{3G} + \Delta t f(\sigma_{eq}) = e_{eq}^m \quad (21)$$

where $f(\sigma_{eq})$ is the nonlinear creep law used in the LIFE Fuel Element Performance computer code [5]. New values of the creep strain increments are calculated from Prandtl-Reuss flow law

$$\Delta e_i^c = \frac{\Delta t f(\sigma_{eq})}{e_{eq}^m} e_i^m \quad (22)$$

If the new values are close enough to the old initial values, the solution is converged. If the new values are not close enough, the process is repeated with the just calculated values serving as the initial guess. By this method they stresses and strains are calculated during the reactor transient.

4. Results

NUFROD results for three LOF coastdown rates are analyzed. The GCFR fuel pin is operating at 27 kW/m with an inlet coolant velocity of 80 m/s. The cladding over the lower 3/4 of the 1.15 m active fuel region is surface roughened. The fuel inner and outer radii are 0.79 mm and 3.25 mm. The cladding inner and outer radii are 3.26 mm and 3.73 mm. A detailed analysis is only performed on the axial segment which from a thermoelastic analysis has the largest stresses.

The first case has a coolant flow coastdown time constant of 1 s. At the axial segment 3/4 down the fuel pin where the largest stresses result, the analysis is performed. Throughout the transient circumferential and axial stresses are about an order of magnitude higher than the radial stress. They are tensile at the inner surface and compressive at the outer surface. Cladding melting causes a slightly shift in the stresses but the dominating circumferential and axial stresses remain large and compressive at the outer fuel surface. Fuel creep relaxes the stresses with time. Figure 1 shows the hoop stress at the fuel outer surface versus time. The hoop stress is always compressive at this outer surface. The spike at about 4 s on the curve of fig. 1 is due to cladding melting. As cladding begins to melt the rate of change of the outer fuel surface temperature decreases. This decrease causes the hoop stress at the outer fuel surface to become less compressive. When the cladding melts and is swept away, the bared outer fuel surface temperature increases rapidly. This increase causes the hoop stress at the outer fuel surface to become more compressive. Fuel creep causes the hoop stress at the outer fuel surface to become less compressive again and tired toward zero stress.

The second case has a coastdown time constant of 10 s. At the same axial location as in the first case, the circumferential and axial stresses initially behave similarly to those in the first case. However at 12 s the outer hoop stress becomes tensile because the thermal strain is no longer an increasing function of radius. This results because the

instantaneous coefficient of linear thermal expansion, α , is an increasing function of temperature, the temperature at the inner surface is so much greater than that at the outer surface, and the temperature change at the outer surface is only slightly larger than that for the inner. Cladding melting and removal send the circumferential and axial stresses at the outer surface back into compression at about 19 s. Figure 2 shows the outer hoop stress versus time for this case. Again the spike on the curve is due to cladding melting.

The results of the third case with a coastdown time constant of 300 s are quite different from the previous two cases. Early in this relatively long transient at about 5 s, the outer circumferential and axial stresses become tensile and remain tensile to the end of the calculation. As explained above, this results because fuel thermal relaxation causes the thermal strain to become a decreasing function of radius. Figure 3 shows the outer hoop stress versus time for this third case.

5. Conclusions

Fission gas in the fuel, the largest amount of which is found in the unrestructured zone, can also affect fuel mechanical response. The stress state of the fuel can evoke various fuel mechanical behaviors in the LOF. Stresses and fission gas can interact to further influence fuel deformation.

In the first case, the fastest transient, the large compressive stresses in the unrestructured zone are expected to limit fuel swelling and prohibit fuel cracking at the outer surface. Fuel melting is expected to be the mode of gross fuel deformation. In the third case, the slowest transient studied, the dominating tensile stresses in the unrestructured zone are expected to increase fuel swelling or fuel cracking, the possible modes of gross fuel deformation.

LOF transients with intermediate coastdown rates may have any of the modes of gross fuel deformation. If fission gas in the unrestructured zone is released from the fuel before tensile stresses act, then fuel cracking at the outer surface may occur. If the fission gas is not released before tensile stresses act, then fuel swelling or fuel cracking may occur.

Cladding melting has been shown to dramatically affect the fuel stresses in the LOF. In some cases, the temperature variations due to cladding melting are responsible for a very rapid change in the sign of the dominating stress. The interactions of fission gas and stress in the LOF need to be studied in greater detail.

6. Acknowledgments

For their technical assistance and encouragement, we thank Michael C. Billone of Northwestern University and Peter K. Mast, James H. Scott, and Jay E. Boudreau of Los Alamos Scientific Laboratory.

References

- [1] A. Mendelson, Plasticity: Theory and Application (MacMillan Co., New York, 1968).
- [2] "Properties for LMFBR Safety Analysis," Argonne National Laboratory report ANL-CEN-RSD-76-1, Supplement 1, LMFBR Safety (UC-79p) (January 1976).
- [3] B. A. Boley and J. H. Weiner, Theory of Thermal Stress (John Wiley & Sons, Inc., New York, 1960).
- [4] M. P. Bohn, "Status Report on Development of FRACAS-II: A Subcode for the Analysis of Fuel and Cladding Deformation," Idaho National Engineering Laboratory report TFBR-TR-151 (December 1976).

[5] V. Z. Jankus and R. W. Weeks, "LIFE-I, A FORTRAN-IV Computer Code for the Prediction of Fast Reactor Fuel Element Behavior," Argonne National Laboratory report ANL-7736 (November 1970).

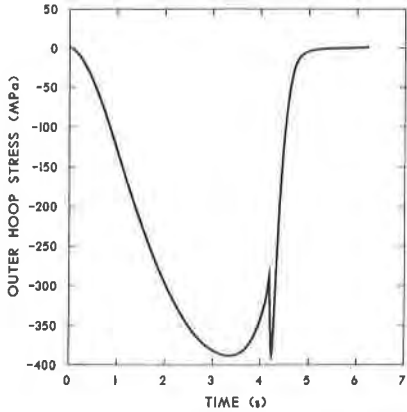


Fig. 1. Hoop stress at fuel outer surface during coolant flow coastdown with 1 s time constant.

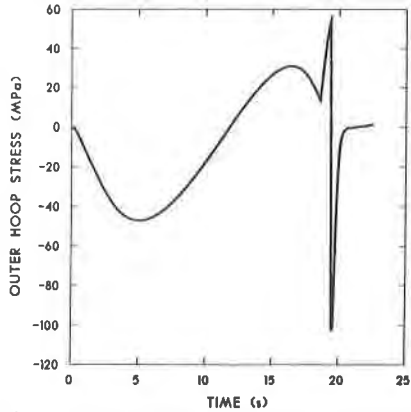


Fig. 2. Hoop stress at fuel outer surface during coolant flow coastdown with 10 s time constant.

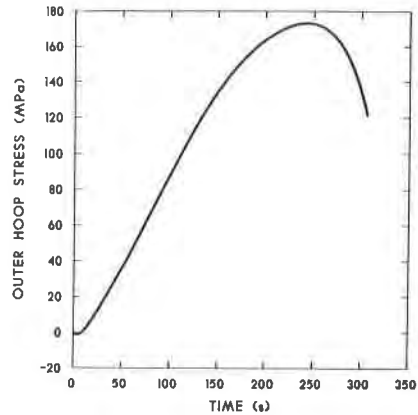


Fig. 3. Hoop stress at fuel outer surface during coolant flow coastdown with 300 s time constant.